

# Validating delta-filters for resonant bar detectors of improved bandwidth foreseeing the future coincidence with interferometers

Sabrina D'Antonio †, Archana Pai ‡, Pia Astone ‡

†INFN Sezione Roma 2 Tor Vergata ITALIA

‡INFN Sezione Roma 1 — P. le Aldo Moro, 2 00185 Roma ITALIA

E-mail: [sabrina.dantonio@lnf.infn.it](mailto:sabrina.dantonio@lnf.infn.it), [archana.pai@roma1.infn.it](mailto:archana.pai@roma1.infn.it),  
[pia.astone@roma1.infn.it](mailto:pia.astone@roma1.infn.it)

**Abstract.** The classical delta filters used in the current resonant bar experiments for detecting GW bursts are viable when the bandwidth of resonant bars is few Hz. In that case, the incoming GW burst is likely to be viewed as an impulsive signal in a very narrow frequency window. After making improvements in the read-out with new transducers and high sensitivity dc-SQUID, the Explorer-Nautilus have improved the bandwidth ( $\sim 20$  Hz) at the sensitivity level of  $10^{-20}/\sqrt{Hz}$ . Thus, it is necessary to reassess this assumption of delta-like signals while building filters in the resonant bars as the filtered output crucially depends on the shape of the waveform. This is presented with an example of GW signals – stellar quasi-normal modes, by estimating the loss in SNR and the error in the timing, when the GW signal is filtered with the delta filter as compared to the optimal filter.

PACS numbers: 04.80 Nn, 07.05 Kf, 97.80 -d

## 1. Introduction

Till date, the burst data analysis in the narrow-band resonant detectors like Explorer-Nautilus is based on the assumption that short gravitational wave(GW) bursts (duration of few millisecond to fraction of a second) appear as delta-like signals in the detector bandwidth (BW). Such an assumption was made mainly because the short GW bursts emit waveforms of unknown shape and further due to detector's narrow band, one could safely assume that the signal emits a flat spectrum in the detector BW. However, recent improvements in resonant bar detectors, mainly the read-out with new transducers and high coupling dc-SQUID [1], have improved the BW ( $\sim 20$  Hz) at the sensitivity level of  $10^{-20}/\sqrt{Hz}$ , see Fig 1(a). Thus, it is important to reassess the above assumption which we demonstrate in this paper with an example of stellar quasi-normal modes (QNM).

Astrophysical inputs indicate [2] that various physical processes can excite stellar QNM during its evolutionary phases, emitting GW in the BW of the resonant bars. Such GW may last for a fraction of a second to few seconds. For example, after the SN core collapse, during the cooling phase, the proto-NS emits GW as a damped sinusoid signal evolving in frequency as well as damping time and can also chirp in the resonant bars [3]‡. In this case, if the data is filtered through a filter matched to a delta-like signal – a delta filter – rather than a proper matched filter, the error in arrival timing as well as loss in SNR can arise. Here, as a preliminary study, we discuss these issues for a simple case of stellar QNM emitting GW  $h(t)$  modeled as a damped sinusoid with a fixed frequency  $f_0 = \omega_0/2\pi$  and damping time  $\tau$ , as given below

$$h(t) = h_0 \sin[\omega_0(t - t_0)] e^{-(t-t_0)/\tau} \theta(t - t_0). \quad (1)$$

Here,  $\theta(t - t_0)$  implies  $h(t) \neq 0$  for  $t \geq t_0$  ( $t_0$  is the time of arrival) and zero otherwise. The damping time  $\tau$  depends on the underlying physical process.

To carry out the delta filter assessment, we assume the signal parameters  $f_0$  and  $\tau$  are known and compare the outputs of the delta filter to that of the matched filter.

## 2. System response

The incoming  $h(t)$  can excite the first longitudinal mode of the resonant bar. A low mass electrical transducer is attached to the bar to convert this displacement of the bar end face into an electrical signal which is further amplified with the SQUID amplifier. Such a bar-transducer system is modeled as a coupled harmonic oscillator with two resonant modes [4]. The  $h(t)$  provides an external force  $f_x(t) = m_x L \ddot{h}(t)/2$  to the bar [ $m_x$ : the reduced mass of the system =  $M_{\text{bar}}/2$ ,  $L$ : the effective length =  $4L_{\text{bar}}/\pi^2$ ].

The electrical output of the transducer is proportional to the relative displacements of the transducer and the bar,  $u(t) = y(t) - x(t)$  from their equilibrium positions. In Fourier domain [4], the response  $u(t)$  to the external force  $f_x(t)$  is obtained by

$$U(j\omega) = W_{ux}(j\omega)F_x(j\omega), \quad (2)$$

‡ Possible candidates for coincidences with interferometers like VIRGO.

where  $W_{ux}(j\omega)$  is the system transfer function from the input force to the output displacement as given defined in Eq.(1.8) of [4]. The  $F_x(j\omega)$  [the FT of  $f_x(t)$ ] for  $h(t)$  defined in Eq. (1) is

$$F_x(j\omega) = \frac{-m_x L \omega^2}{2} H(j\omega) = \frac{-m_x h_0 L \omega^2}{2} \frac{\omega_0 \tau^2}{(1 + j\omega\tau)^2 + \tau^2 \omega_0^2} \exp(-j\omega t_0) \quad (3)$$

where  $H(j\omega)$  is the FT of  $h(t)$ . The  $|F_x(j\omega)|$  is a Lorentzian which becomes narrower (broader), and in(de)creases in height as  $\tau$  in(de)creases, see Fig. 1(a). Conveniently, we choose  $t_0 = 0$ . The relative displacement of the transducer  $u(t)$  is in units of length. The electrical signal at the output of the SQUID amplifier is then given by

$$v(t) = K u(t) \equiv M_v u_0(t) \quad \text{in units of V,} \quad (4)$$

where  $M_v \equiv K M_u$  and  $M_u$  is the maximum value of  $u(t)$  §.

The expected power spectral density (PSD) of the noise  $n(t)$  at the output of the electrical chain is given by [4]

$$S_t(\omega) = S_n + \alpha^2 S_{fx} |W_{ux}(j\omega)|^2 + \alpha^2 S_{fy} |W_{uy}(j\omega)|^2. \quad (5)$$

The  $S_n$  is the broad-band noise contribution from the SQUID and the electrical chain with a flat spectrum in the BW and the rest is the narrow-band noise contribution – due to the thermal noise of the two mechanical oscillators. The  $S_{fx}$  and  $S_{fy}$  is the total noise force spectra due to the Nyquist and the back-action force. The  $W_{ux}$  and  $W_{uy}$  are the system transfer functions as defined in [4] ||.

### 3. Matched filter

Signal detection problem involves computing a statistic – a functional of the data  $z(t)$  – which when passed through the threshold allows to make the decision of either presence [i.e.  $z(t) = n(t) + v(t)$ ] or absence of signal [i.e.  $z(t) = n(t)$ ] in the data.

For known signal in Gaussian-stationary noise, matched filtering is the optimal filtering. The matched filter output is given by

$$o(t) \equiv \langle z, q \rangle = \frac{1}{2\pi} \int_{-\infty}^{\infty} Z(j\omega) Q(j\omega) \exp(j\omega t) d\omega. \quad (6)$$

The matched filter transfer function for  $v(t)$  is  $Q(j\omega) = N_u U_0^*(j\omega) / S_t(\omega)$  with  $U_0(j\omega)$  as the FT of  $u_0(t)$ . The normalization  $N_u = [\frac{1}{2\pi} \int_{-\infty}^{\infty} |U_0(j\omega)|^2 / S_t(\omega) d\omega]^{-1}$  is such that  $\text{Max} \langle u_0, q \rangle = 1$ . In no noise case,  $z(t) = v(t)$  and

$$o(t) = \langle v, q \rangle = \frac{M_v}{2\pi} \int_{-\infty}^{\infty} \frac{N_u |U_0(j\omega)|^2}{S_t(\omega)} \exp(j\omega t) d\omega. \quad (7)$$

Thus, using the above normalization, we obtain  $\text{Max}[o(t)] = M_v$ , from which one can estimate the strength of the input GW  $h_0$ . The matched filter SNR can be evaluated as  $\text{SNR}^2 = (\text{Max}[o(t)])^2 / \text{Var}(\langle n, q \rangle)$ . The variance of the filtered noise is given by

$$\text{Var}(\langle n, q \rangle) = E\{\langle n, q \rangle^2\} - (E\{\langle n, q \rangle\})^2 = N_u. \quad (8)$$

§  $K$  is equal to  $\alpha AB$  of Ref. [4] which includes SQUID amplification and transducer constants.

|| Besides, the other spurious unknown noise sources are treated while filtering the data.

Thus, the matched filter SNR is given by ¶

$$\text{SNR}_M^2 = \frac{M_v^2}{N_u} = \frac{1}{2\pi} \int_{-\infty}^{\infty} \frac{|V(j\omega)|^2}{S_t(\omega)} d\omega, \quad (9)$$

where  $V(j\omega)$  is the FT of  $v(t)$ . In terms of the signal and system poles  $p_i, i = 1, \dots, 6$

$$p_1 = -\omega_+ + j/\tau_+, p_2 = -p_1^*, p_3 = -\omega_- + j/\tau_-, p_4 = -p_3^*, p_5 = -\omega_0 + j/\tau, p_6 = -p_5^*, \quad (10)$$

and the decay times  $\tau_+, \tau_-$  pertaining to the response of the two modes [i.e.  $f_{\pm}, \omega_{\pm} = 2\pi f_{\pm}$ ] at the output of the delta filter  $^+$ , the  $\text{SNR}_M$  is

$$\text{SNR}_M^2 = \frac{-h_0^2 L^2 \omega_0^2 K^2}{16S_n} \Re \left[ \frac{\tau_+ p_1^7}{\omega_+ \prod_{i,i \neq 1,2} (p_1^2 - p_i^2)} + \frac{\tau_- p_3^7}{\omega_- \prod_{i,i \neq 3,4} (p_3^2 - p_i^2)} + \frac{\tau p_5^7}{\omega_0 \prod_{i,i \neq 5,6} (p_5^2 - p_i^2)} \right].$$

#### 4. Explorer-Nautilus Delta filter

As stated earlier, the delta-filtering is the most natural approach for detecting unknown short GW bursts in the narrow-band detector. The delta filters are developed as follows.

The normalized system response to a delta-like signal (used to build the delta-filter) is  $u^\delta(t)$  such that  $U^\delta(j\omega) = W_{ux}/M_\delta$  [4] and  $\text{Max}[u^\delta(t)] = 1$ . Then, the delta filter, constructed from this response has the transfer function  $Q^\delta(j\omega) = N_\delta U^{\delta*}(j\omega)/S_t(\omega)$  with the filter normalization  $N_\delta = [\frac{1}{2\pi} \int_{-\infty}^{\infty} |U^\delta(j\omega)|^2/S_t(\omega) d\omega]^{-1}$ . This filter construction is such that if an impulse is incident on the bar with  $v(t) = M_v u^\delta(t)$  then the maximum of the filtered output  $\text{Max}(\langle v, q^\delta \rangle)$  is  $M_v$ .

However, when the response of the detector to the damped sinusoid is filtered through the delta filter, the filtered output becomes

$$\begin{aligned} o(t) &= \langle v, q^\delta \rangle = \frac{M_v}{2\pi} \int_{-\infty}^{\infty} \frac{N_\delta U_0(j\omega) U^{\delta*}(j\omega)}{S_t(\omega)} \exp(j\omega t) d\omega, \\ &= \frac{-h_0 L \omega_0 K N_\delta}{4\pi S_n M_\delta} \int_{-\infty}^{\infty} \frac{\omega^4 \exp(j\omega t) d\omega}{(\omega^2 - p_1^2)(\omega^2 - p_2^2)(\omega^2 - p_3^2)(\omega^2 - p_4^2)(\omega - p_5)(\omega - p_6)}. \end{aligned}$$

We solve this integration by applying the residue theorem and obtain

$$\begin{aligned} o(t) &= \frac{-h_0 L \omega_0 K N_\delta}{8S_n M_\delta} \Re \left[ -\frac{\tau_+ e^{-t/\tau_+}}{\omega_+} \frac{p_1^5 e^{-j\omega_+ t}}{\prod_{i=3,4} (p_1^2 - p_i^2) \prod_{k=5,6} (p_1 - p_k)} \right. \\ &\quad \left. - \frac{\tau_- e^{-t/\tau_-}}{\omega_-} \frac{p_3^5 e^{-j\omega_- t}}{\prod_{i=1,2} (p_3^2 - p_i^2) \prod_{k=5,6} (p_3 - p_k)} + \frac{j e^{-t/\tau}}{\omega_0} \frac{p_5^6 e^{-j\omega_0 t}}{\prod_{i=1,\dots,4} (p_5^2 - p_i^2)} \right] \quad (11) \end{aligned}$$

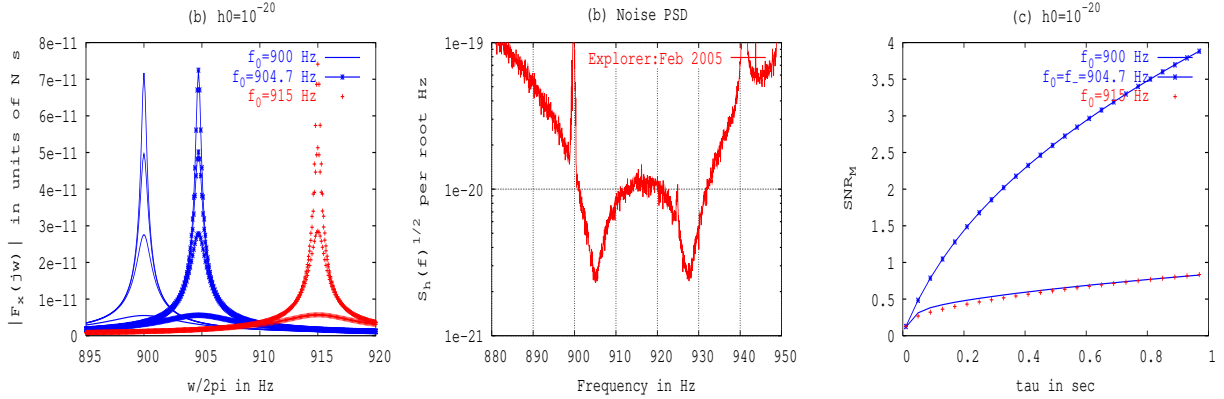
The variance of the filtered noise is  $\text{Var}(\langle n, q^\delta \rangle) = N_\delta$ . Thus,

$$\text{SNR}_\delta^2 = \frac{M_v^2}{N_\delta} (\text{Max} \langle u_0, q^\delta \rangle)^2. \quad (12)$$

#### 5. Comparison and Numerical plots

To illustrate, we use the parameters pertaining to Explorer[Feb 2005]; two resonant frequencies  $f_- = 904.7$  Hz,  $f_+ = 927.452$  Hz,  $\tau_+ \sim 140$  ms,  $\tau_- \sim 150$  ms,  $K \sim$

**Figure 1.** (a)  $|F(j\omega)|$  vs  $f$  for  $\tau = 50, 250, 450, 650$  ms, the higher peak corresponds to higher  $\tau$ . (b) Explorer : Two sided PSD in per  $\sqrt{\text{Hz}}$ , (c)  $\text{SNR}_M$  vs  $\tau$  for  $h_0 \sim 10^{-20}$ .



$1.66 \times 10^{13} \text{V/m}$  and  $S_n \sim 10^{-8} \text{V}^2/\text{Hz}$ . Fig.1(b) shows the noise PSD of Explorer. The BW of the detector at the level of  $\sqrt{S_n} \sim 10^{-20}/\sqrt{\text{Hz}}$  is  $\sim 20$  Hz and we define the sensitive frequency band as FB :  $\{900, 932\}$ . We note that at  $f \sim 915$  Hz, the sensitivity is the worst within FB. We divide our study in 2 cases, (a)  $f_0 \in \text{FB}$ , (b)  $f_0$  far from FB.

Fig.1(c) shows the plot of  $\text{SNR}_M$  vs  $\tau$  for fixed  $h_0 \sim 10^{-20}$ . As  $\tau$  increases  $\text{SNR}_M$  increases as the signal spends more time in the detector. However, for  $f_0$  close to  $f_{\pm}$ , this increase is sharp as the incoming  $h(t)$  excites the resonances and gives more and more energy to  $f_{\pm}$  as  $\tau$  increases, see Fig.1(a). For a given  $\tau$ , the difference in SNR's of two incoming GW with frequencies  $f_-$  and 915 Hz is related to the corresponding  $S_h(f_-)$  and  $S_h(915)$  [see Fig.1(b)]. In Fig.1(c), the SNR for  $f_0 = 900$  Hz and  $f_0 = 915$  Hz are similar as the detector sensitivity is similar at those frequencies. For  $f_0$  away from the resonance, the detector band falls in the tail of the signal Lorentzian giving small power to the resonances even at high  $\tau$ . Thus, the increase in SNR is very slow in such case. The similar plot can be obtained fixing the signal energy instead of  $h_0$ . However, the signal energy of QNM is itself a function of  $\tau$ . Thus, for clear demonstration of dependence of SNR on  $\tau$ , we fix  $h_0$  here.

### 5.1. $\text{SNR}_M$ vs $\text{SNR}_\delta$

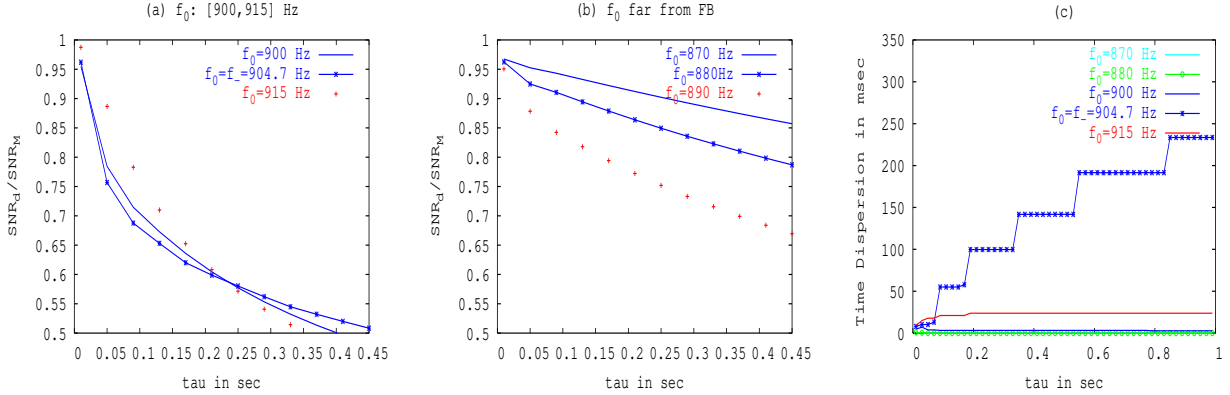
To validate the delta filter, we study the loss in SNR when the signal is filtered with the delta filter, i.e. the ratio between Eq.(12) and Eq.(9). In Fig. 2, we plot this ratio for case (a) and (b) respectively. We show that when  $f_0 \in \text{FB}$ , the  $\text{SNR}_\delta$  is comparable to that of the  $\text{SNR}_M$  (assuming the SNR loss of  $\sim 15\%$ ) for all  $\tau < 50$  ms. This loss increases as  $\tau$  increases. Thus, when  $f_0 \in \text{FB}$ , for high  $\tau$ , the delta filter is far from optimal. Contrarily, when  $f_0$  is far from FB, the tail of the signal Lorentzian gives relatively flat spectrum in detector BW (for small values of  $\tau$ ), similar to a delta-like signal. Consequently, delta filter matches the signal giving  $\text{SNR}_M$  comparable to that

¶ For detailed discussion, see [5]

+ In [4],  $\tau_+, \tau_-$  are indicated by  $\tau_{3+}, \tau_{3-}$  respectively,

of  $\text{SNR}_\delta$  for  $\tau$  as large as  $\sim 200$  ms. However, as  $\tau$  increases, due to the nature of signal Lorentzian, the energy given to both the resonances is not the same. This results in the decrease in SNR ratio as  $\tau$  increases even for case (b). This loss is related to the error in the estimation of  $h_0$ . However, we note that in case(b), the  $\text{SNR}_M$  is well below the  $\text{SNR}_M$  obtained for case(a) for the same  $h_0$ .

**Figure 2.** SNR loss in (a) Case (a), (b) Case (b), (c) Error in timing



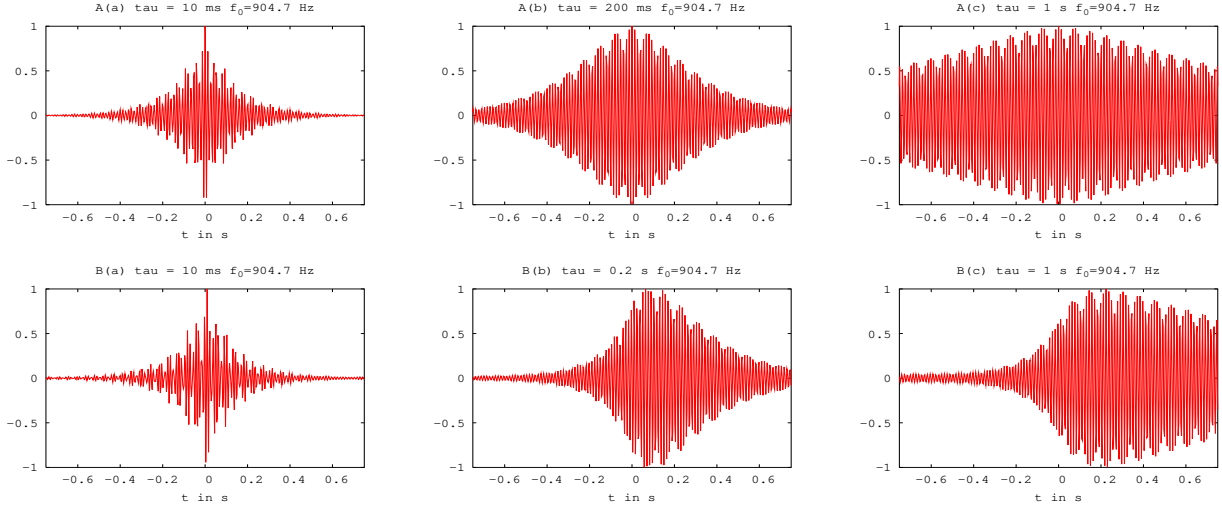
## 5.2. Arrival timing error

In Fig. 3, we plot the output of the delta as well as matched filter for case (a) with  $f_0 = f_-$  and  $\tau = 0.01, 0.2, 1$  s. We show in Fig. 3 A (a), when  $\tau < \tau_\pm$ , the decay of the matched filtered output is dominated by the  $\tau_\pm$  ( $\sim 140$ ms). However, as  $\tau$  increases and is  $> \tau_\pm$  [see Fig 3 A (b) and (c)], the decay time of the filtered output is dominated by the signal term which can increase the arrival timing error. However, it is worth noting that with the noise, this error not only depends on the decay time of the filtered output but also on the SNR. As  $\tau$  increases, the decay time increases but at the same time the  $\text{SNR}_M$  also increases (which we wish to investigate in future with simulations).

The output of the delta filter is shown in Fig.3 B. The output is asymmetric about  $t = t_0 = 0$  as the delta filter is causal [as it is not properly matched] unlike the matched filter. Mathematically, it can be seen by the the relative sign difference between the signal term and the two resonances in Eq.(11). In this case, the filtered output becomes maximum when  $t \sim t_0 + \tau$ . Thus, the arrival timing error is proportional to  $\tau$ , see fig. 2 (c). The steps correspond to the beating frequency which in general depends on  $f_0$  and  $f_\pm$ . In this case when  $f_0 = f_-$ , it is  $(f_+ - f_-)/2 \sim 12$  Hz. We note that this beating is crucial while fixing the coincidence timing window while performing coincidences between say Explorer-Nautilus or Explorer-Virgo.

In case (b), when  $f_0$  is far away from FB, the situation is contrary. In this case, the timing error is small, [see Fig. 2 (c)]. As explained earlier, for  $f_0$  away from FB and low  $\tau$ , the signal acts as a delta-like signal. As a result, delta-filter itself is a matched filter hence gives no timing error. Mathematically, the signal term in Eq.(11) is small compared to other terms.

**Figure 3.** Normalized output of the (A) matched filter, (B) delta filter, for  $\tau = 10\text{ms}, 0.2\text{s}, 1\text{s}$  and  $f_0 = f_-$ .



## 6. Conclusion

In this work, we did a comparative study of the response of the matched filter *vs* delta-filters for filtering the damped sinusoids GW signals for resonant bar detectors. We divided our study in two cases: (a)  $f_0 \in \text{FB}$  and (b)  $f_0$  far from the FB with  $\text{FB} = \{900, 932\}$  using Explorer configuration. We find that in case (a), the loss in SNR increases as  $\tau$  and so does the arrival timing error if delta-filter is used instead of matched filter. However, in case (b), the signal almost acts like a delta for small  $\tau$  hence the SNR loss is negligible for small  $\tau$  however as  $\tau$  increases, the SNR loss gradually increases. The arrival timing error is minimal for all  $\tau$ . Thus, we can optimally use delta filters for detecting signals in case (b) for  $\tau$  as large as 200 ms. But, to detect damped sinusoids in case (a) with  $\tau$  as large as 50 ms, it is mandatory to use the optimal filtering as opposed to delta-filter. This poses a problem of setting an “optimal” grid of templates in  $f_0, \tau$  when  $f_0, \tau$  are fixed. However, as described earlier,  $f_0$  and  $\tau$  can evolve in the detector bandwidth. For detecting such signals and perform coincidences, the delta filter is inadequate and an optimal “matched” filter is difficult to construct due to insufficient knowledge of signal waveform. Alternative detection methods are needed which we pursue in future work.

## Acknowledgments

AP would like to thank INFN for financial support, and ICTP, LNF for the hospitality.

- [1] P. Astone, *et. al* Phys. Rev. Lett. **91** 111101 (2003), gr-qc/0307120.
- [2] N. Andersson and K. D. Kokkotas (2004), gr-qc/0403087.
- [3] V. Ferrari, G. Miniutti and J. A. Pons, Mon. Not. R. Astro. Soc. **342**, 629 (2003).
- [4] P. Astone, C. Buttiglione, S. Frasca, G. V. Pallotino and G. Pizzella, Nuovo Cim. C **20**, 9 (1997).
- [5] A. Pai, C. Celsi, G. V. Pallotino, S. D’Antonio and P. Astone, *in Preparation*